Astronomy & Astrophysics manuscript no. pmn_x-ray
March 3, 2022
©ESO 2022

arXiv:1501.00790v1 [astro-ph.HE] 5 Jan 2015

A redshifted Fe Kα line from the unusual γ-ray source PMN J1603−4904

C. Müller[1,2], F. Krauß[1,2], T. Dauser[2], A. Kreikenbohm[1,2], T. Beuchert[1,2], M. Kadler[1], R. Ojha[3,4,5], J. Wilms[2], M. Böck[1,2,6], B. Carpenter[4,5], M. Dutka[4], A. Markowitz[7,2], W. McConville[4], K. Pottschmidt[3,4], Ł. Stawarz[8,9], and G. B. Taylor[10]

[1] Institut für Theoretische Physik und Astrophysik, Universität Würzburg, Am Hubland, 97074 Würzburg, Germany
e-mail: cornelia.mueller@astro.uni-wuerzburg.de
[2] Dr. Remeis Sternwarte & ECAP, Universität Erlangen-Nürnberg, Sternwartstrasse 7, 96049 Bamberg, Germany
[3] Center for Space Science and Technology, University of Maryland Baltimore County, Baltimore, MD 21250, USA
[4] CRESST and NASA, Goddard Space Flight Center, Astrophysics Science Division, Code 661, Greenbelt, MD 20771, USA
[5] Catholic University of America, Washington, DC 20064, USA
[6] Max-Planck-Institut für Radioastronomie, Auf dem Hügel 69, 53121 Bonn, Germany
[7] University of California, San Diego, Center for Astrophysics and Space Sciences, 9500 Gilman Drive, La Jolla, CA 92093-0424, USA
[8] Institute of Space and Astronautical Science JAXA, 3-1-1 Yoshinodai, Chuo-ku, Sagamihara, Kanagawa 252-5210, Japan
[9] Astronomical Observatory, Jagiellonian University, ul. Orla 171, Kraków 30-244, Poland
[10] Department of Physics and Astronomy, University of New Mexico, Albuquerque, NM 87131, USA

March 3, 2022

ABSTRACT

Context. Multiwavelength observations have revealed the highly unusual properties of the γ-ray source PMN J1603−4904, which are difficult to reconcile with any other well established γ-ray source class. The object is either a very atypical blazar or compact jet source seen at a larger angle to the line of sight.
Aims. In order to determine the physical origin of the high-energy emission processes in PMN J1603−4904, we study the X-ray spectrum in detail.
Methods. We performed quasi-simultaneous X-ray observations with *XMM-Newton* and *Suzaku* in 2013 September, resulting in the first high signal-to-noise X-ray spectrum of this source.
Results. The 2–10 keV X-ray spectrum can be well described by an absorbed power law with an emission line at 5.44 ± 0.05 keV (observed frame). Interpreting this feature as a Kα line from neutral iron, we determine the redshift of PMN J1603−4904 to be $z = 0.18 \pm 0.01$, corresponding to a luminosity distance of 872 ± 54 Mpc.
Conclusions. The detection of a redshifted X-ray emission line further challenges the original BL Lac classification of PMN J1603−4904. This result suggests that the source is observed at a larger angle to the line of sight than expected for blazars, and thus the source would add to the elusive class of γ-ray loud misaligned-jet objects, possibly a γ-ray bright young radio galaxy.

Key words. Galaxies: active – Galaxies: jets – Galaxies: individual: PMN J1603−4904 – X-rays: galaxies – Gamma rays: galaxies

1. Introduction

Active Galactic Nuclei (AGN) are among the brightest extragalactic sources at X-ray energies. According to the unification model (Antonucci 1993; Urry & Padovani 1995), the orientation of AGN with respect to the line of sight, different accretion rates, and the presence of a powerful jet lead to different spectral appearances. Jet-dominated sources at the smallest jet inclination angles are classified as blazars. Sources which are oriented at larger angles to the line of sight are typically less dominated by beamed jet emission. The origin of the X-ray emission of radio-loud AGN is still an open question (e.g., Fukazawa et al. 2014). It can arise from Comptonization of seed photons from the accretion disc in the hot corona, synchrotron or inverse Compton emission, or a combination of these. The most prominent emission line in AGN X-ray spectra is the Fe Kα line at ∼6.4 keV (e.g., Nandra 2006; Shu et al. 2010; Ricci et al. 2014). This line is usually explained by fluorescence of neutral or mildly ionized iron produced by the primary, hard X-ray photons irradiating the accretion disk or the molecular torus. Measurements of iron line emission probe therefore the inner regions of AGN. The detection of an iron line is a clear indication of reprocessed radiation from matter in the vicinity of the primary X-ray source. Iron lines are common features in spectra of radio-quiet and radio-loud sources at larger jet angles to the line of sight (Bianchi et al. 2004). In contrast, typical blazar X-ray spectra are featureless continua, clearly dominated by the beamed jet emission that outshines any putative underlying emission components (e.g., Rivers et al. 2013; Grandi et al. 2006).

In Müller et al. (2014, hereafter Mue14), we discussed the multiwavelength properties of PMN J1603−4904, which is associated with a bright γ-ray source with a remarkably hard spectrum (2FGL J1603.8–4904; Nolan et al. 2012). These properties are difficult to reconcile with its original classification as a BL Lac type blazar (Nolan et al. 2012; Ackermann et al. 2013): High resolution TANAMI (Ojha et al. 2010) radio observations using Very Long Baseline Interferometry (VLBI) revealed

a symmetric structure on milliarcsecond (mas) scales with the brightest, most compact component at the center. The broadband spectral energy distribution (SED) showed an excess in the infrared, which could be modeled with a blackbody spectrum with $T \sim 1600$ K, consistent with the emission of circumnuclear dust heated by the disk photons. Such thermally reprocessed radiation is not expected in typical blazar SEDs. Optical measurements constrained the redshift to $z \lesssim 4.24$ (Shaw et al. 2013). Based on the results presented by Mue14, however, no conclusive classification of PMN J1603−4904 could be made. While *Swift*/XRT observations showed a faint X-ray counterpart, low photon statistics did not allow us to sufficiently constrain its X-ray spectrum.

In this letter, we report on the first *XMM-Newton* and *Suzaku* observations of PMN J1603−4904 conducted within the scope of the TANAMI multiwavelength program (Sect. 2). In Sect. 3 we present the X-ray spectral characteristics and discuss its implications in Sect. 4.

2. Observations and data reduction

In 2013 September, we performed quasi-simultaneous X-ray observations of PMN J1603−4904 with *XMM-Newton* (Jansen et al. 2001, obs-id 0724700101, performed 2013-09-17) and *Suzaku* (Koyama et al. 2007, obs-id 708035010, performed 2013-09-13) in order to constrain the X-ray spectrum better than previous observations with *Swift*/XRT (Burrows et al. 2005, Mue14). The *XMM-Newton* data processing, analysis, and extraction of the spectrum were performed using the standard tasks of the *XMM System Analysis Software* (SAS 13.5.0). We detected a single, unresolved, X-ray source at the radio position of PMN J1603−4904. Only data from EPIC-PN (Strüder et al. 2001, exposure time 39.0 ks) and EPIC-MOS 1 (Turner et al. 2001, exposure time 33.4 ks) cameras were used, as the usable exposure of EPIC-MOS 2 was only 4.7 ks. The PN spectrum was extracted using a circle with 35″ radius centered on the coordinates of the radio source. For the background spectrum a circular source-free region of 50″ radius was chosen. For the MOS 1 data extraction, background and source regions with radii of 100″ were used. We chose larger extraction radii for the background to minimize the measurement uncertainty. We used the HEASOFT v6.15 package for the *Suzaku* data analysis. Extraction and background regions of 94″ were used for all XIS detectors, which after filtering had an exposure time of 48.5 ks. The spectral analysis was performed using the *Interactive Spectral Interpretation System* (ISIS, Version 1.6.2-27, Houck & Denicola 2000). An independent analysis of the *XMM-Newton* and *Suzaku* data revealed no significant flux variability during the observed period. In order to improve the statistics and ensure the validity of the χ^2-statistics, all 1–10 keV spectra were rebinned to a minimum signal-to-noise ratio of 5 and modeled simultaneously considering the background. Throughout this paper we use the standard cosmological model with $\Omega_m = 0.3$, $\Lambda = 0.7$, $H_0 = 70\,\mathrm{km\,s^{-1}\,Mpc^{-1}}$ (Beringer et al. 2012). All uncertainties quoted in the following are given at the 90% confidence.

3. Results

3.1. X-Ray continuum

The quasi-simultaneous data from *XMM*/PN, MOS 1, and *Suzaku*/XIS were simultaneously modeled with an absorbed power-law component, a Gaussian emission line, and cross-calibration constants to account for the relative flux calibrations

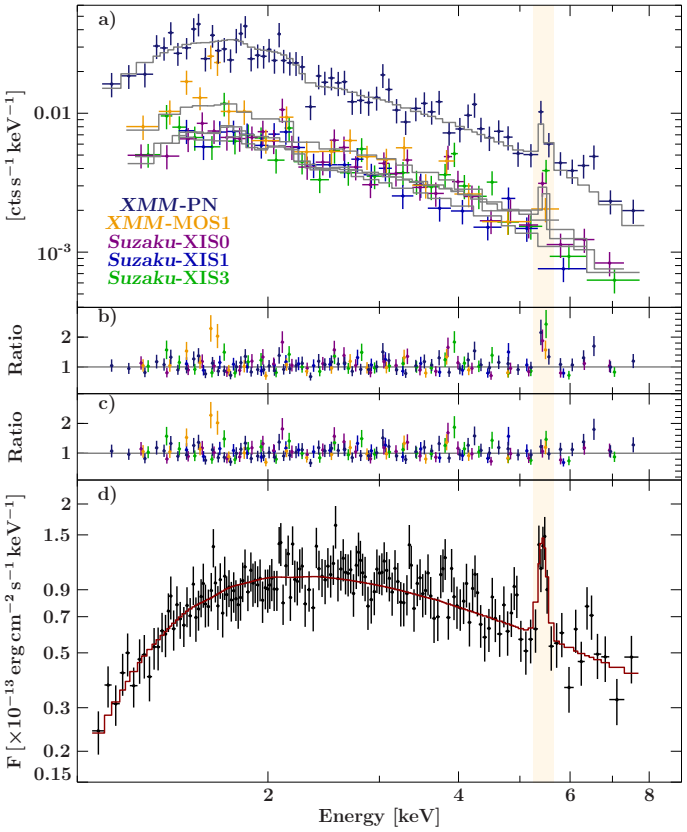


Fig. 1. Simultaneous fit to the *XMM-Newton* and *Suzaku* data (see Table 1). The data are best fitted by an absorbed power-law component with an emission line at $\sim 5.44 \pm 0.05$ keV. *(a):* Count spectrum for all detectors fitted with an absorbed power law and a Gaussian emission line (models shown in gray). Ratio of data to model for a fit of an absorbed power law (*b*) and including a Gaussian emission line (*c*). *(d):* Unfolded, combined spectrum of all data sets with the best-fit model (red). The shaded region highlights the position of the emission line.

of the instruments. We use the `tbnew` model (Wilms et al. 2012) to account for neutral Galactic absorption (Galactic HI value is fixed to $N_H = 6.32 \times 10^{21}\,\mathrm{cm^{-2}}$; Kalberla et al. 2005), and the cross sections and abundances of Verner et al. (1996) and Wilms et al. (2000), respectively. Further residuals reveal the presence of source intrinsic absorption, which we model with an additional, redshifted absorption component (`tbnew_z`, see below). We detect a strong emission line that can be modeled by a Gaussian component at 5.44 ± 0.05 keV with an equivalent width of $EW = 200 \pm 90$ eV (Fig. 1a). Using the centroid energy of the Gaussian emission line with respect to the neutral Fe Kα line line rest frame energy, we can constrain the redshift of the system to $z = 0.18 \pm 0.01$ (see Sect. 3.2 for details). We find a photon index of $\Gamma_X = 2.07^{+0.04}_{-0.12}$ with an intrinsic absorption of $N_H = 2.05^{+0.14}_{-0.12} \times 10^{22}\,\mathrm{cm^{-2}}$. The best fit model parameters can be found in Table 1. Adding a Gaussian line to describe the emission line improves the fit from $\chi^2 = 198.1$ (165 degrees of freedom [dof]) to $\chi^2 = 183.3$ (162 dof). To test for the significance of the line feature at 5.44 keV, we performed a Monte Carlo simulation based on the Null-Hypothesis that the intrinsic model for the measured counts is an absorbed power-law lacking a line. This hypothesis is rejected with a p-value of $p < 1.1 \times 10^{-4}$. Figure 1 shows the spectra of all single datasets with the best fit model and the combined datasets regridded to a joint energy grid.

Table 1. Best fit parameters using an absorbed power-law model with a Gaussian emission line.

Parameter	Value
$N_{\rm H}$ (intrinsic)	$2.05^{+0.14}_{-0.12} \times 10^{22}$ cm^{-2}
$F_{2-10\,\rm keV}$ (de-absorbed)	$(4.39 \pm 0.17) \times 10^{-13}$ erg s^{-1} cm^{-2}
Γ	$2.07^{+0.04}_{-0.12}$
$E_{\rm Fe\ K\alpha}$	5.44 ± 0.05 keV
$\sigma_{\rm Fe\ K\alpha}$	< 0.06 eV
EW	200 ± 90eV
const$_{\rm pn}$	1.0
const$_{\rm MOS1}$	$1.00^{+0.09}_{-0.08}$
const$_{\rm XIS0}$	1.57 ± 0.11
const$_{\rm XIS1}$	1.46 ± 0.12
const$_{\rm XIS3}$	1.63 ± 0.12
χ^2/dof	183.0/162

3.2. Iron emission line

Due to its high fluorescent yield, the Fe Kα transition produces the most prominent line feature in the 2–10 keV energy range. Such lines are seen in the X-ray spectra of the majority of Seyfert and radio galaxies (de La Calle Pérez et al. 2010). In most sources where redshifts are known (e.g., Markowitz et al. 2007; Shu et al. 2010; Ricci et al. 2014), the line energy and equivalent width are consistent with an origin by fluorescence with rest-frame energy of ∼6.4 keV in a neutral to mildly ionized medium that is irradiated by hard X-rays. Even in sources showing relativistically broadened Fe Kα lines from the innermost regions of the accretion disk, narrow line components consistent with a rest-frame energy of 6.4 keV are typically seen (Risaliti et al. 2013; Marinucci et al. 2014a,b). We therefore consider it most probable that the emission line seen in PMN J1603−4904 at 5.44 ± 0.05 keV is also emitted intrinsically at 6.4 keV[1], such that the corresponding redshift of the source can be constrained to $z = 0.18 \pm 0.01$.

Adopting this redshift, the luminosity distance is 872 ± 54 Mpc. In the rest-frame, the intrinsic X-ray luminosity, neglecting Galactic and source intrinsic absorption, is $L_{2-10\,\rm keV} = (4.03 \pm 0.20) \times 10^{43}$ erg s^{-1} and the γ-ray luminosity is $L_{1-100\,\rm GeV} = (8.1 \pm 1.1) \times 10^{45}$ erg s^{-1} (for $S_{1-100\,\rm GeV} = (1.44 \pm 0.07) \times 10^{-10}$ erg s^{-1} cm^{-2}, Nolan et al. 2012). At 8.4 GHz, we derive a rest-frame luminosity density of $L_{8.4\,\rm GHz} = (7.3 \pm 1.5) \times 10^{32}$ ergs^{-1} Hz^{-1} (based on the flux from Mue14). The comparison of ATCA observations at arcsec resolution and VLBI observations with milliarcsecond resolution shows that ∼80% of the radio emission is emitted on scales of ∼15 mas (Mue14), i.e., ∼46 pc at $z = 0.18$. The remaining ∼20% is emitted on larger scales which are constrained to $\lesssim 1''$ (Mue14), i.e., ∼3 kpc at $z = 0.18$.

4. Discussion

The X-ray properties derived from the *XMM-Newton* and *Suzaku* spectra allow us to further constrain the classification of this unusual γ-ray source. Here we compare the X-ray spectrum of PMN J1603−4904 to the typical spectra of different radio-loud AGN (see Table 2).

Compared to other source types, blazars are the most luminous AGN at the X-ray energies (e.g., Chang 2010; Rivers et al. 2013). With an X-ray luminosity of $L_{2-10\,\rm keV} \sim 4 \times 10^{43}$ erg s^{-1}, PMN J1603−4904 is only comparable to the fainter blazars of the BL Lac type. Its γ-ray luminosity of $L_\gamma \sim 8 \times 10^{45}$ erg s^{-1} is comparable to low or intermediate peaked[2] BL Lac objects and flat spectrum radio quasars (Ackermann et al. 2011). Since blazar X-ray spectra are dominated by beamed jet emission, they are generally featureless[3] and can in most cases be modeled with a simple or broken power law (Chang 2010; Ushio et al. 2010; Rivers et al. 2013). The strong iron line in the X-ray spectrum of PMN J1603−4904 therefore suggests a non-blazar nature. The intrinsic X-ray absorption ($N_{\rm H} \sim 2{\times}10^{22}$ cm^2) is furthermore unusually high compared to other blazars (Kubo et al. 1998; Chang 2010; Rivers et al. 2013). We therefore conclude that its original classification as a BL Lac (Nolan et al. 2012; Shaw et al. 2013) is very unlikely.

The multiwavelength properties of PMN J1603−4904 opened the door to an alternative classification as a jet source seen at a larger inclination angle, i.e., a radio galaxy (Mue14). Overall, the X-ray properties of PMN J1603−4904 are comparable to those of radio galaxies (Table 2). In about 50% of all broad-line radio galaxies, Fe Kα lines with equivalent widths of typically a few 100 eV are detected (e.g., Sambruna et al. 1999). PMN J1603−4904 has a comparable equivalent width of $EW = 200 \pm 90$ eV. We caution, however, that only few non-blazar sources are detected at γ-ray energies (Abdo et al. 2010; Nolan et al. 2012; Katsuta et al. 2013). The γ-ray luminosities of such "misaligned" jets show a broad range from $L_\gamma \sim 10^{41}$–10^{46} erg s^{-1}, with FR I galaxies being typically less γ-ray luminous than FR II sources. The γ-ray luminosity of PMN J1603−4904 is only comparable to the most powerful misaligned sources (Abdo et al. 2010).

Among the sources seen at a large inclination angle, Compact Steep Spectrum (CSS) and Gigahertz Peaked Spectrum (GPS) sources can be interpreted as the younger versions of evolved radio galaxies, often showing compact symmetric object (CSO) radio morphologies at parsec scales (Readhead et al. 1996a,b; O'Dea 1998). Owing to its milliarcsecond-scale properties, we discussed the possible classification of PMN J1603−4904 as a CSO in Mue14. The 2–10 keV spectra of GPS and CSO sources can generally be well modeled by absorbed power laws (e.g., Vink et al. 2006; Guainazzi et al. 2006; Siemiginowska et al. 2008; Tengstrand et al. 2009; Kunert-Bajraszewska et al. 2014). Fe Kα emission is only detected in a few sources (e.g., Guainazzi et al. 2006; Siemiginowska 2009; Tengstrand et al. 2009). The X-ray properties of PMN J1603−4904 are a good match to the findings in these sample studies of GPS and CSS sources. These sources generally have a radio luminosity density of $L \gtrsim 10^{32}$–10^{36} erg s^{-1} Hz^{-1} at 5 GHz (O'Dea & Baum 1997, for combined complete samples). Thus PMN J1603−4904 is compatible with the less powerful GPS and CSS sources. Its linear size is comparable to the canonical size limit for CSOs (< 1 kpc) or medium-size symmetric objects (< 15 kpc; Fanti et al. 1995; Readhead 1995; Readhead et al. 1996b). Gamma-ray emission was predicted from theoretical modeling of GPS sources (e.g., Stawarz et al. 2008;

[1] In the very unlikely event that the line is instead due to emission from a strongly ionized plasma, for hydrogen-like iron, the Lyα resonance at 6.966 keV would yield a redshift of $z = 0.28 \pm 0.01$.

[2] The synchrotron peak frequency derived from the parametrization of the broadband spectral energy distribution is $\nu_{\rm sync} \simeq 2.2 \times 10^{12}$ Hz (Mue14), which would be more in line with a low-peaked object (defined by $\nu^S_{\rm peak} < 10^{14}$ Hz; Fossati et al. 1998; Donato et al. 2001).

[3] As a rare exception, Grandi & Palumbo (2004) discuss the detection of a narrow Fe Kα line in the flat-spectrum radio quasar 3C 273. In this case the thermal (unbeamed) and the beamed jet emission could be disentangled due to source variability, suggesting the presence of an underlying Seyfert-like component (Soldi et al. 2008).

Ostorero et al. 2010; Kino et al. 2013; Migliori et al. 2014) and first source candidates have been discussed, e.g., 4C +55.17 (McConville et al. 2011) with similar broadband properties as PMN J1603−4904. If confirmed as a γ-ray loud young radio galaxy, then PMN J1603−4904 would be a well-suited object to investigate the origin of high-energy emission.

5. Conclusions

We have presented new X-ray observations of PMN J1603−4904, which further challenge its previous classification as a blazar and strongly suggest that this jet system is seen at a larger inclination angle to the line of sight. Its X-ray spectrum can be modeled by an absorbed power law and a Gaussian emission line at 5.44 ± 0.05 keV, and can be best explained as emission from a non-blazar source. These X-ray properties are consistent with a young or evolved radio galaxy. We interpret the significantly detected spectral line as a neutral Fe Kα line with rest frame energy 6.4 keV. This identification results in the first redshift measurement for this source of $z = 0.18 \pm 0.01$, i.e., a luminosity distance of 872 ± 54 Mpc.

PMN J1603−4904 is associated with a hard spectrum γ-ray source (Nolan et al. 2012)[4]. If it is indeed seen at a larger inclination angle where the observed emission is less intensified by Doppler boosting than in blazars, it adds to the class of so-called misaligned sources rarely detected at γ-ray energies (Abdo et al. 2010), with a remarkably high γ-ray luminosity.

Further multiwavelength observations are required to confirm PMN J1603−4904 as a γ-ray loud young radio galaxy: VLBI monitoring will allow us to check for proper motion in opposite directions with respect to the core. Low radio frequency observations could help to determine a putative peak at $\lesssim 1$ GHz, thus increasing confidence in its identification as a GPS source, and to constrain the extended radio emission.

Acknowledgements. We thank the referee for the helpful comments, and R. Schulz and P.G. Edwards for the useful discussions that improved the manuscript. C.M. acknowledges the support of the Bundesministerium für Wirtschaft und Technologie (BMWi) through Deutsches Zentrum für Luft- und Raumfahrt (DLR) grant 50 OR 1404 and of the Studienstiftung des Deutschen Volkes. This research was funded in part by the National Aeronautics and Space Administration (NASA) through Fermi Guest Investigator grants NNH09ZDA001N, NNH10ZDA001N, and NNH12ZDA001N, by BMWi through DLR grant 50 OR 1311, by Deutsche Forschungsgemeinschaft grant WI1860/10-1, and by an appointment to the NASA Postdoctoral Program at the Goddard Space Flight Center, administered by Oak Ridge Associated Universities through a contract with NASA. We thank J. E. Davis for the development of the `slxfig` module that has been used to prepare the figure in this work. This research has made use of ISIS functions provided by ECAP/Dr. Karl Remeis-Observatory (Bamberg, Germany) and MIT (http://www.sternwarte.uni-erlangen.de/isis/).

References

Abdo, A. A., Ackermann, M., Ajello, M., et al. 2010, ApJ, 720, 912
Ackermann, M., Ajello, M., Allafort, A., et al. 2011, ApJ, 743, 171
Ackermann, M., Ajello, M., Allafort, A., et al. 2013, ApJS, 209, 34
Antonucci, R. 1993, ARA&A, 31, 473
Beringer, J., Arguin, J.-F., Barnett, R. M., et al. 2012, Phys. Rev. D, 86, 010001
Bianchi, S., Matt, G., Balestra, I., Guainazzi, M., & Perola, G. C. 2004, A&A, 422, 65
Burrows, D. N., Hill, J. E., Nousek, J. A., et al. 2005, Space Sci. Rev., 120, 165
Chang, C.-S. 2010, PhD thesis, Max-Planck-Institut für Radioastronomie, Bonn, Germany
de La Calle Pérez, I., Longinotti, A. L., Guainazzi, M., et al. 2010, A&A, 524, A50
Donato, D., Ghisellini, G., Tagliaferri, G., & Fossati, G. 2001, A&A, 375, 739
Eracleous, M., Sambruna, R., & Mushotzky, R. F. 2000, ApJ, 537, 654
Evans, D. A., Worrall, D. M., Hardcastle, M. J., Kraft, R. P., & Birkinshaw, M. 2006, ApJ, 642, 96
Fanti, C., Fanti, R., Dallacasa, D., et al. 1995, A&A, 302, 317
Fossati, G., Maraschi, L., Celotti, A., Comastri, A., & Ghisellini, G. 1998, MNRAS, 299, 433
Fukazawa, Y., Finke, J., Stawarz, L., et al. 2014, ApJ, in press
Grandi, P., Malaguti, G., & Fiocchi, M. 2006, ApJ, 642, 113
Grandi, P. & Palumbo, G. G. C. 2004, Science, 306, 998
Guainazzi, M., Siemiginowska, A., Stanghellini, C., et al. 2006, A&A, 446, 87
Hardcastle, M. J., Evans, D. A., & Croston, J. H. 2006, MNRAS, 370, 1893
Houck, J. C. & Denicola, L. A. 2000, in Astronomical Data Analysis Software and Systems IX, ed. N. Manset, C. Veillet, & D. Crabtree, Astron. Soc. Pacific Conf. Ser. 216, 591
Jansen, F., Lumb, D., Altieri, B., et al. 2001, A&A, 365, L1
Kalberla, P. M. W., Burton, W. B., Hartmann, D., et al. 2005, A&A, 440, 775
Katsuta, J., Tanaka, Y. T., Stawarz, Ł., et al. 2013, A&A, 550, A66
Kino, M., Ito, H., Kawakatu, N., & Orienti, M. 2013, ApJ, 764, 134
Koyama, K., Tsunemi, H., Dotani, T., et al. 2007, PASJ, 59, 23
Kubo, H., Takahashi, T., Madejski, G., et al. 1998, ApJ, 504, 693
Kunert-Bajraszewska, M., Labiano, A., Siemignowska, A., & Guainazzi, M. 2014, MNRAS, 437, 3063
Marinucci, A., Matt, G., Kara, E., et al. 2014a, MNRAS, 440, 2347
Marinucci, A., Matt, G., Miniutti, G., et al. 2014b, ApJ, 787, 83
Markowitz, A., Takahashi, T., Watanabe, S., et al. 2007, ApJ, 665, 209
McConville, W., Ostorero, L., Moderski, R., et al. 2011, ApJ, 738, 148
Migliori, G., Siemiginowska, A., Kelly, B. C., et al. 2014, ApJ, 780, 165
Müller, C., Kadler, M., Ojha, R., et al. 2014, A&A, 562, A4
Nandra, K. 2006, MNRAS, 368, L62
Nolan, P. L., Abdo, A. A., Ackermann, M., et al. 2012, ApJS, 199, 31
O'Dea, C. P. 1998, PASP, 110, 493
O'Dea, C. P. & Baum, S. A. 1997, AJ, 113, 148
Ojha, R., Kadler, M., Böck, M., et al. 2010, A&A, 519, A45
Ostorero, L., Moderski, R., Stawarz, Ł., et al. 2010, ApJ, 715, 1071
Readhead, A. C. S. 1995, Proc. NAS, 92, 11447
Readhead, A. C. S., Taylor, G. B., Pearson, T. J., & Wilkinson, P. N. 1996a, ApJ, 460, 634
Readhead, A. C. S., Taylor, G. B., Xu, W., et al. 1996b, ApJ, 460, 612
Ricci, C., Ueda, Y., Ichikawa, K., et al. 2014, A&A, 567, A142
Risaliti, G., Harrison, F. A., Madsen, K. K., et al. 2013, Nat, 494, 449
Rivers, E., Markowitz, A., & Rothschild, R. 2013, ApJ, 772, 114
Sambruna, R. M., Eracleous, M., & Mushotzky, R. F. 1999, ApJ, 526, 60
Shaw, M. S., Romani, R. W., Cotter, G., et al. 2013, ApJ, 764, 135
Shu, X. W., Yaqoob, T., & Wang, J. X. 2010, ApJS, 187, 581
Siemiginowska, A. 2009, AN, 330, 264
Siemiginowska, A., LaMassa, S., Aldcroft, T. L., Bechtold, J., & Elvis, M. 2008, ApJ, 684, 811
Soldi, S., Türler, M., Paltani, S., et al. 2008, A&A, 486, 411
Stawarz, L., Ostorero, L., Begelman, M. C., et al. 2008, ApJ, 680, 911
Strüder, L., Briel, U., Dennerl, K., et al. 2001, A&A, 365, L18
Tengstrand, O., Guainazzi, M., Siemiginowska, A., et al. 2009, A&A, 501, 89
Turner, M. J. L., Abbey, A., Arnaud, M., et al. 2001, A&A, 365, L27
Urry, C. M. & Padovani, P. 1995, PASP, 107, 803
Ushio, M., Stawarz, Ł., Takahashi, T., et al. 2010, ApJ, 724, 1509
Verner, D. A., Ferland, G. J., Korista, K. T., & Yakovlev, D. G. 1996, ApJ, 465, 487
Vink, J., Snellen, I., Mack, K.-H., & Schilizzi, R. 2006, MNRAS, 367, 928
Wilms, J., Allen, A., & McCray, R. 2000, ApJ, 542, 914
Wilms, J., Juett, A. M., Schulz, N. S., & Nowak, M. A. 2012, available at `http://pulsar.sternwarte.uni-erlangen.de/wilms/research/tbabs/`

[4] Note that a small possibility of a false association of the γ-ray source with PMN J1603−4904 still remains, although in such a case an even more exotic explanation for the γ-ray origin would be required.

Table 2. Typical high-energy spectral parameters for different source classes compared to results for PMN J1603−4904.

	Blazars	Radio Galaxies	GPS/CSS	PMN J1603−4904
$L_{2-10\mathrm{keV}}$ [erg s^{-1}]	$\sim 10^{43}$–10^{46}[a]	$\sim 10^{42}$–10^{45}[b]	10^{42}–10^{46}[c]	$(4.03 \pm 0.20) \times 10^{43}$
L_γ [erg s^{-1}]	10^{44}–10^{49}[d]	$\sim 10^{41}$–10^{46}[d]	–	$(8.1 \pm 1.1) \times 10^{45}$
$\Gamma_{2-10\,\mathrm{keV}}$	1.4–2.5[e]	1.7–1.8[f]	1.7–2.0[g]	$2.07^{+0.04}_{-0.12}$
N_H (intrinsic) [cm^{-2}]	$\lesssim 10^{21}$[e]	$\sim 10^{21}$–10^{24}[f]	$\sim 10^{22}$[h]	$2.05^{+0.14}_{-0.12} \times 10^{22}$
Fe Kα line	no[e]	yes[e]	yes[i]	yes
$EW_{\mathrm{Fe\,K}\alpha}$ [eV]	–	[e]	$\lesssim 150$[i]	200 ± 90

Notes. [a] Chang (2010, for the radio flux density-limited MOJAVE 1 sample) [b] Sambruna et al. (1999) [c] Vink et al. (2006), Siemiginowska et al. (2008). [d] Abdo et al. (2010), Ackermann et al. (2011). [e] Sambruna et al. (1999), Chang (2010), Rivers et al. (2013). [f] Sambruna et al. (1999), Eracleous et al. (2000), Evans et al. (2006), Hardcastle et al. (2006), Grandi et al. (2006), Rivers et al. (2013). [g] Siemiginowska et al. (2008). [h] Vink et al. (2006), Guainazzi et al. (2006), Siemiginowska et al. (2008), Tengstrand et al. (2009), Kunert-Bajraszewska et al. (2014). [i] Guainazzi et al. (2006), Siemiginowska (2009), Tengstrand et al. (2009).